Reconstitution of Membrane Proteins into Giant Unilamellar Vesicles via Peptide-Induced Fusion

Kahya, Nicoletta; Pécheur, Eve-Isabelle; Boeij, Wim P. de; Wiersma, Douwe A.; Hoekstra, Dick

Published in:
Biophysical Journal

DOI:
10.1016/S0006-3495(01)75801-8

Reconstitution of Membrane Proteins into Giant Unilamellar Vesicles via Peptide-Induced Fusion

Nicoletta Kahya,* Eve-Isabelle Pécheur,† Wim P. de Boeij,* Douwe A. Wiersma,* and Dick Hoekstra†
*Ultrafast Laser and Spectroscopy Laboratory, Optical Sciences, Materials Science Centre, University of Groningen, Nijenborgh 4, 9747 AG Groningen, The Netherlands and †Department of Membrane Cell Biology, University of Groningen, Antonius Deusinglaan 1, 9713 AV Groningen, The Netherlands

ABSTRACT In this work, we present a protocol to reconstitute membrane proteins into giant unilamellar vesicles (GUV) via peptide-induced fusion. In principle, GUV provide a well-defined lipid matrix, resembling a close-to-native state for biophysical studies, including optical microspectroscopy, of transmembrane proteins at the molecular level. Furthermore, reconstitution in this manner would also eliminate potential artifacts arising from secondary interactions of proteins, when reconstituted in planar membranes supported on solid surfaces. However, assembly procedures of GUV preclude direct reconstitution. Here, for the first time, a method is described that allows the controlled incorporation of membrane proteins into GUV. We demonstrate that large unilamellar vesicles (LUV, diameter 0.1 μm), to which the small fusogenic peptide WAE has been covalently attached, readily fuse with GUV, as revealed by monitoring lipid and contents mixing by fluorescence microscopy. To monitor contents mixing, a new fluorescence-based enzymatic assay was devised. Fusion does not introduce changes in the membrane morphology, as shown by fluorescence correlation spectroscopy. Analysis of fluorescence confocal imaging intensity revealed that ~6 to 10 LUV fused per μm^2 of GUV surface. As a model protein, bacteriorhodopsin (BR) was reconstituted into GUV, using LUV into which BR was incorporated via detergent dyalisis. BR did not affect GUV-LUV fusion and the protein was stably inserted into the GUV and functionally active. Fluorescence correlation spectroscopy experiments show that BR inserted into GUV undergoes unrestricted Brownian motion with a diffusion coefficient of 1.2 μm^2/s. The current procedure offers new opportunities to address issues related to membrane-protein structure and dynamics in a close-to-native state.

INTRODUCTION

Many processes and reactions occurring in cellular membranes are regulated by the lateral organization and dynamic behavior of both lipids and proteins. An important question, still debated in biology, is whether or not lipid segregation takes place in the plane of the membrane to form microdomains or "rafts" (Simons and Ikonen, 1997; Harder and Simons, 1997). An appealing hypothesis for the biological role of rafts is that lipid aggregation in a submicron scale may concentrate interacting species in particular regions and/or regulate protein dynamics. Moreover, the lateral mobility and oligomeric organization of many membrane proteins are crucial to their activity. The interplay of the dynamic properties of both lipidic and proteic membrane components is thought to be important for the regulation of several complex machineries such as those responsible for signal transduction, membrane transport and trafficking (Van Voorst and Kruijff, 2000; Simons and Toomre, 2000).

Recent developments in optical microscopy can provide valuable additional insight into the structure/function relationship of membrane proteins. In particular, fluorescence correlation spectroscopy (FCS; Eigen and Rigler, 1994) may serve this purpose as it allows determination of single-molecule diffusion, chemical kinetics, conformational equilibrium, and aggregation-dissociation behavior. Single particle tracking (SPT) (Ghosh and Webb, 1994; Schmidt et al., 1996) has been applied extensively to studies of lateral motion of single lipid molecules in artificial membranes (Schmidt et al., 1995; Sonnleitner et al., 1999) and, only recently, SPT has been successfully used for studies of lipid rafts in vivo (Schutz et al., 2000). An important development for further investigations in this direction would be the insertion of membrane proteins into artificial membranes, which allows observations of diffusion, oligomeric state, and conformation of membrane proteins as a function of the lipid composition of the membrane.

Given the molecular complexity of biological systems, membrane reconstitution is an increasingly important approach to delineate the properties of a protein in a lipid bilayer (Camilli and Warren, 1999). To apply single-molecule spectroscopy to membrane proteins embedded in an artificial membrane, vesicles with a radius of at least 2 to 3 μm are required. However, correct and controlled insertion of functional transmembrane proteins into such artificial bilayers still constitutes a problem. In recent years, supported planar membranes (Tamm and Kalb, 1993; Sackmann, 1996) have been used extensively to study properties of lipids and membrane-bound proteins. These membrane systems, however, suffer from severe artifacts because of the presence of a rigid support, glass or quartz, that interacts with the exposed soluble domains and thereby changes artificially the mobility of proteins in the membrane (Wagner and Tamm, 2000).

Received for publication 2 November 2000 and in final form 22 May 2001.
Address reprint requests to Dr. Nicoletta Kahya, Optical Sciences, University of Groningen, Nijenborgh 4, 9747 AG, Groningen, The Netherlands. Tel.: 31-50-3634324; Fax: 31-50-3634441; E-mail: kahya@chem.rug.nl.

0006-3495/01/09/1464/11 $2.00

Giant unilamellar vesicles (GUV) provide free-standing bilayers, without any substrate effect, and, therefore, such membranes are potentially very attractive model systems (Angelova and Dimitrov, 1986; Dimitrov and Angelova, 1988). However, the fragility and protein-hostile preparation procedures of these large vesicles have so far precluded their use in membrane reconstitution.

In this work, we present a novel procedure to efficiently reconstitute transmembrane proteins into GUV, while fully preserving the activity of the protein. The protein is first incorporated in submicron vesicles, large unilamellar vesicles (LUV), which then fuse with GUV via a peptide-induced fusion mechanism previously developed for LUV-LUV fusion (Pécheur et al., 1997, 1999). As a model system, we use bacteriorhodopsin (BR), but the technique has been applied to other proteins as well (unpublished results). We show that the proton-pumping activity of BR is retained after the transfer to the GUV, and that the protein undergoes an unrestricted lateral motion in the plane of the membrane. This procedure provides a valuable tool in structure/function studies of transmembrane proteins, as analyzed by single-molecule optical microscopic techniques.

MATERIALS AND METHODS

Chemicals

L-α-Dioleoyl-phosphatidylcholine (DOPC), L-α-dioleoyl-phosphatidylethanolamine (DOPE), cholesterol (chol), and L-α-dipalmitoyl-phosphatidylethanolamine (DPPE) were purchased from Avanti Polar Lipids (Alabaster, AL). *N*-Succinimidyl 3-(2-pyridyldithio)-propionate (SPDP)-derivatized DPPE (PE-PDP) was synthesized as previously described (Martin et al., 1999). Purity and stability of PE-PDP were checked by thin-layer chromatography. SAINT-2 (1-methyl-4, 19-*cis*, *cis*-heptatritiaconta-9, 28-dienylpyridinium chloride), a cationic amphiphile, was synthesized as described elsewhere (Woude et al., 1997). WAE (N-Trp-Ala-Glu-Ser-Leu-Gly-Glu-Ala-Leu-Glu-Cys) was synthesized and purified to >95% purity by Syntem (Nîmes, France). The peptide was dissolved in 20 mM ammonium bicarbonate at pH 8 and stored at −20°C. *N*-(Lissamine rhodamine B sulfonyl) dihexadecanoyl-*sn*-glycero-3-phosphoethanolamine (*N*-Rh-PE); *N*-(fluorescein-5-thiocarbamoyl)-1,2-dihexadecanoyl-*sn*-glycero-3-phosphoethanolamine, triethylammonium salt (fluorescein DHPE); rhodamine green-labeled dextran (MW 3000); Alexa Fluor 488 carboxylic acid; succinimidyl ester (Alexa Fluor 488 reactive dye); fluorescein di-β-D-galactopyranoside (FDG); Texas Red 1,2-dihexadecanoyl-*sn*-glycero-3-phosphoethanolamine, triethylammonium salt (Texas Red DHPE); and 8-hydroxypyrene-1,3,6-trisulfonic acid, trisodium salt (pyranine) were purchased from Molecular Probes (Leiden, the Netherlands). β-D-Galactoside galactohydrolase (β-galactosidase); *n*-octyl-β-D-glucopyranoside (*n*-octyl glucoside, OG); poly-L-lysine (0.1% w/v in water); and valinomycin were from Sigma (St. Louis, MO). Sephadex G25 columns (PD-10) were obtained from Amersham Pharmacia Biotech (Uppsala, Sweden) and SM_2 Bio-Beads from Bio-Rad (Hercules, CA). All other reagents were of analytical grade.

Preparation of LUV

Liposomes were prepared by freeze-thawing, followed by extrusion. Briefly, lipids in chloroform/methanol (9:1 v:v) solutions were mixed, dried under nitrogen and suspended in water, unless otherwise stated. They were then submitted to 10 cycles of freezing into liquid nitrogen and thawing in a waterbath at 50°C, which was followed by extrusion through 0.1- or 0.4-μm polycarbonate membranes. Unless indicated otherwise, LUV were composed of DOPC/chol/PE-PDP (3.5:1.5:0.25); in some experiments 1% *N*-Rh-PE was included. The peptide WAE was then coupled via the C-terminal cysteine to the LUV by an overnight conjugation at 4°C. The molar ratio PE-PDP:peptide of 1:5 produced a coupling efficiency of 10 to 20%, as evaluated by measuring spectrophotometrically at 343 nm the amount of the reaction product, 2-mercaptopyridine (Pécheur et al., 1997). The peptide-coupled liposomes were purified by gel filtration through a Sephadex G25 column, thereby removing unbound peptide.

Preparation of GUV

GUV were prepared by the electroformation technique (Angelova and Dimitrov, 1986; Dimitrov and Angelova, 1988). With this approach, GUV are produced varying in size from 10 to 100 μm, as demonstrated by freeze-fracture electron microscopy and statistical analysis of thermal undulations (Menger and Angelova, 1998). The homogeneity of the size distribution depends on the lipid composition and buffer conditions (Mathivet et al., 1996). The chamber for vesicle preparation was composed of two microscope slides, each coated with a thin layer of indium tin oxide, which made them optically transparent and electrically conductive. Lipids (DOPC/DOPE/SAINT-2, 10:3:0.65 or 10:3:1.3 molar ratio) in chloroform/methanol (9:1) were deposited on the indium tin oxide glass plates and the solvent was evaporated under vacuum. The sealant paste Sigillum wax (Vitrex, Copenhagen, Denmark), of 1-mm thickness, was used as a spacer between the two plates. After adding water into the chamber (~300 μl), a voltage of 1.1 V at 10 Hz frequency was applied for 2 to 3 h through thin metal electrodes, sealed on the glass plates.

Assays for monitoring lipid and protein mixing during vesicle fusion

After the addition of the peptide-coupled LUV to the chamber of GUV, lipid mixing was assayed by monitoring the fluorescence distribution of *N*-Rh-PE (λ_{ex} = 560 nm, λ_{em} = 590 nm), initially inserted into the LUV (1 mol%). Note that the GUV contained the positively charged SAINT-2 as a target lipid for the negatively charged peptide. Protein-lipid mixing of the reconstituted proteoliposomes (LUV, see below) was assayed similarly. In this case, LUV contained Alexa Fluor 488-labeled BR (see Labeling of BR in Materials and Methods), allowing the transfer of the protein to be monitored at λ_{ex} = 488 nm and λ_{em} = 519 nm. In both cases, fluorescence images were taken with a microscope (Axiovert S100 TV, Carl Zeiss Inc., Thornwood, NY), equipped with a Zeiss NeoFluor 40×, NA = 0.75 objective or a Zeiss CP-Achromat 100×, NA = 1.25 oil immersion objective and a CCD camera (Hamamatsu C5985; Bridgeport, NJ).

Assays for monitoring contents mixing during vesicle fusion

Internal contents mixing during GUV-LUV fusion were assayed in two ways. In one procedure, we prepared LUV (5–10 μl of 5 mM vesicle suspension) containing water-soluble rhodamine green-labeled dextran (5 mM, final concentration) and monitored its transfer into the lumen of the GUV (300 μl of 0.1 mM vesicle suspension) upon fusion. Fluorescence images were recorded with the microscope (Zeiss NeoFluor 40×, NA = 0.75 objective) equipped with a charge coupled device (CCD) camera (Hamamatsu C5985).

Alternatively, a more sensitive procedure was developed, based upon the selective cleavage of a fluorogenic carbohydrate substrate by a glycosidase. Thus, 2 to 3 units of β-galactosidase were entrapped in LUV (400 nm-sized, 5–10 μl of a 5 mM lipid suspension), which were added to the

GUV (300 μl of 0.1 mM of lipid suspension), containing 10 mM FDG, prepared in 20 mM Tris-HCl, pH 7.6. After the mixing of contents, hydrolysis of the substrate FDG in the lumen of the GUV causes the release of the fluorescein dye. The mixing of the contents was followed by monitoring the increase of the fluorescence, attributable to enzymatic turnover, with the microscope (Zeiss NeoFluor 40×, NA = 0.75 objective), equipped with a CCD camera.

Confocal imaging for quantification of GUV-LUV fusion efficiency

The fusion events between LUV and GUV were quantified by confocal imaging. Confocal images were obtained by focusing the excitation light of an Ar ion laser (Coherent Inc., Santa Clara, CA) at 488 nm into a 15-μm pinhole spatial filter. The spatially filtered light was deflected by a dichroic mirror (500 dichroic longpass (DCLP)) and focused by the objective (Zeiss C-Apochromat 63×, NA = 1.2 water immersion) in an inverted microscope (Axiovert S100 TV, Zeiss) into the sample. The fluorescence signal was sent to the detector, an avalanche photodiode (EG&G Optoelectronics, Vaudreuil, Quebec, Canada). A 15-μm pinhole in front of the detector eliminated the out-of-focus contributions, allowing a confocal sectioning of the sample. An OG515 filter in the detection arm filtered out the scattered excitation light.

Fluorescence intensity analysis was obtained by calibrating the detection setup with a sample of 100-nm liposomes containing 2% of fluorescein DHPE. The liposomes were fixed on glass coverslips coated with poly-L-lysine. The excitation power was kept low to prevent photobleaching (1 μW). First, calibration was done by determining the fluorescence intensity of a single LUV. As the size of the LUV is beyond the optical resolution, only the total intensity of each LUV can be measured (average intensities of 320,000 counts/s). After fusion (10 min incubation at room temperature), and following elimination of those LUV that had not fused by flushing the flow chamber (Warner Instruments RC-21; Hamden, CT), in which the experiments were carried out, confocal images of the GUV were taken under the same experimental conditions as for the LUV imaging. The equatorial slice of the imaged GUV was 1 μm thick (the point spread function in this confocal geometry was measured with PS-speck 175 nm yellow-green beads [Molecular Probes] in water). Intensities of 2,000,000 up to 2,800,000 counts/s were measured per point from a 1-μm thick slice. At the laser power used, no photobleaching occurred during the imaging and the fluorescence signal was assumed proportional to the number of dye molecules present (no self-quencing). Due to the flexibility of the dye molecule with respect to the lipids, orientational effects on the detection yield average out. By dividing the intensities measured for GUV and LUV, the number of LUV fused can thus be calculated.

Membrane reconstitution of BR into LUV

BR from *Halobacterium halobium* was membrane-reconstituted into LUV using octyl-β-D-glucoside dyalisis, as described earlier (Rigaud et al., 1988). Briefly, purple membrane was isolated and BR purified by a modification of the procedure of Oesterhelt and Stoeckenius (1974; Dencher and Heyn, 1982); BR was solubilized in a 100 mM octyl glucoside solution in 25 mM phosphate buffer, pH 6.9, at a detergent-to-protein ratio of 20 (w/w). After sonication for 20 s, the sample was incubated in the dark at 35°C for 1 h and then at room temperature for 20 h. Solubilization was confirmed by the inability of BR to sediment after centrifugation at 200,000 × *g* for 1 h. The quality of the preparation was checked by spectrophotometry; the solubilizate did not contain aggregates and only trace amounts of free retinal were present.

Octyl glucoside was added to the liposome suspension in a 10-to-1 detergent-to-lipid molar ratio (50 mM OG/5 mM lipid), and after 5 to 10 min of incubation, BR (50 to 500 μg/ml) was added. The detergent-lipid-protein mixture was kept at room temperature, while gently stirring for 15 min, after which the detergent was removed by dialysis (Philippot et al., 1983). Bio-Beads were placed outside the dialysis bag (9 mg of Bio-Beads for 1 μmol of detergent) to remove the detergent from the medium. The proteoliposomes were separated from nonincorporated material by gel filtration. The degree of reconstitution was determined by absorbance measurements at 560 nm (ϵ_{560} = 54000 M^{-1} cm^{-1}), giving a final reconstituted protein concentration of 50 to 450 μg/ml.

Labeling of BR

BR was labeled with Alexa Fluor 488 either before reconstitution in the monomeric detergent-state or after reconstitution. Conjugation was performed by reacting the succinimidyl ester moiety of the dye with the primary amines present in the protein in bicarbonate buffer at pH 8. The protein conjugate was then separated from unreacted dye by gel filtration; the degree of labeling amounted 0.8 to 1.0 of bound dye molecules per BR. Labeling efficiency and fusion yields were found to be comparable using either labeling procedure.

Assay for the activity of BR in GUV

Changes in the pH of the GUV's lumen, because of the proton pumping of the reconstituted BR, were measured as changes in the fluorescence intensity of the membrane-impermeable, pH-sensitive probe pyranine (Rigaud et al., 1988). BR was reconstituted into WAE-coupled LUV suspended in 20 mM 1,4-piperazinediethanesulfonic acid (PIPES), 110 mM K_2SO_4, pH 7.2, and containing 1% of Texas Red DHPE. The LUV were fused to GUV prepared in 20 mM PIPES, pH 7.2, 200 μM pyranine, and 100 nM valinomycin. Fusion was checked by monitoring lipid mixing under the microscope as the Texas Red DHPE (λ_{ex} = 582 nm and λ_{em} = 601 nm) diffused in the GUV's membrane. After 30 min illumination with a xenon lamp, a decrease in pH inside the GUV, caused by the proton pumping activity of BR, was observed with the microscope as the fluorescence intensity of pyranine entrapped in the GUV decreased. This decrease allows to discriminate GUV-entrapped pyranine from nonentrapped probe, which was left in the medium.

Fluorescence correlation spectroscopy measurements

The experimental setup consisted of a CW Ar ion laser operating at 488 nm. The laser beam was directed via a dichroic mirror and a 63× NA = 1.2 water immersion objective (Zeiss C-Apochromat) to the sample (2–5 μW laser power in the back aperture of the objective), and the fluorescence was collected by the same objective and imaged onto a 30-μm pinhole located in front of an avalanche photodiode (EG&G Optoelectrics). An OG515 filter placed in the detection arm filtered out the excitation light, backscattered from the sample. The signal was sent to a PCI-6602, 80 MHz counter card (National Intruments, austin, TX) and then to a computer where the algorithm for the autocorrelation curve was applied. To measure the lateral mobility of the lipid and the protein in the membrane, a two-dimensional diffusional model was used (Magde et al., 1972). The setup was calibrated by imaging PS-speck 175 nm yellow-green beads (Molecular Probes) in water.

RESULTS

Lipid mixing occurs during GUV-LUV interaction

For a controlled insertion of a transmembrane protein into GUV, it is essential to prove that LUV and GUV fully fuse. As it has been shown that the undecameric peptide WAE,

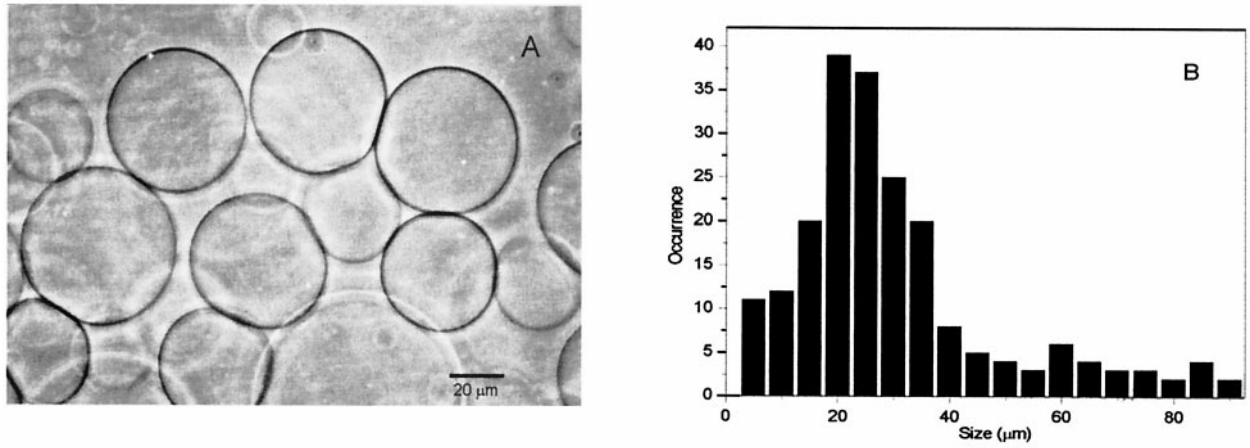

FIGURE 1 (*A*) Phase-contrast image of GUV (DOPC/DOPE/SAINT-2 10:3:1.3) in water. A Zeiss CP-Achromat 40×, Phase Contrast 2 objective was used. (*B*) Size distribution of a population of GUV (DOPC/DOPE/SAINT-2 10:3:1.3) in water. Liposomes with a diameter <5 μm were not counted.

even at low concentrations, is an efficient fusogen for LUV-LUV fusion (Pécheur et al., 1997), we used WAE-coupled vesicles for GUV-LUV fusion. Given its small size (e.g., compared with that of a viral fusion protein), it is not likely that the peptide will interfere with the reconstituted protein or perturb its optical or spectroscopic properties. Further, in order to promote the association between GUV and WAE-coupled vesicles, the cationic lipid SAINT-2 was included in the GUV, as it will provide a positively-charged interaction site for the negatively charged peptide. DOPE was also included as a lipid because it favors negative bilayer curvature, a parameter that strongly promotes protein-induced membrane fusion (Zimmerberg et al., 1993; Pécheur et al., 1997).

GUV composed of DOPC/DOPE/SAINT-2 were prepared by the electroformation technique with a DOPC:DOPE ratio of 10:3, while the amount of SAINT-2 was varied between 5 and 30%. With this composition, and by applying a voltage of 1.1 V at 10 Hz for 2–3 h, mainly spherical GUV were obtained with diameter varying from 10 to 100 μm (Fig. 1, *A* and *B*). Presumably because of its charge, the presence of the cationic SAINT-2 promoted the process of vesicle growth. When freshly prepared, no thermal undulations were apparent, implying a good tensile strength. However, after a few hours at room temperature, the GUV began to undulate with a bending elasticity modulus typical of unilamellar bilayers.

Lipid mixing, as indicated by the transfer of nonexchangeable *N*-Rh-PE between WAE-coupled LUV and GUV, was readily observed with the microscope. Immediately after mixing (Fig. 2 *A*), a patchy appearance of fluorescence along the rims of the GUV was observed, reflecting the attachment of numerous *N*-Rh-PE-labeled LUV. This patchy appearance transformed, for $>90\%$ of the GUV, into a smoother and more continuous ring-like appearance over a time course of $\sim$15 to 20 min (Fig. 2 *B*),

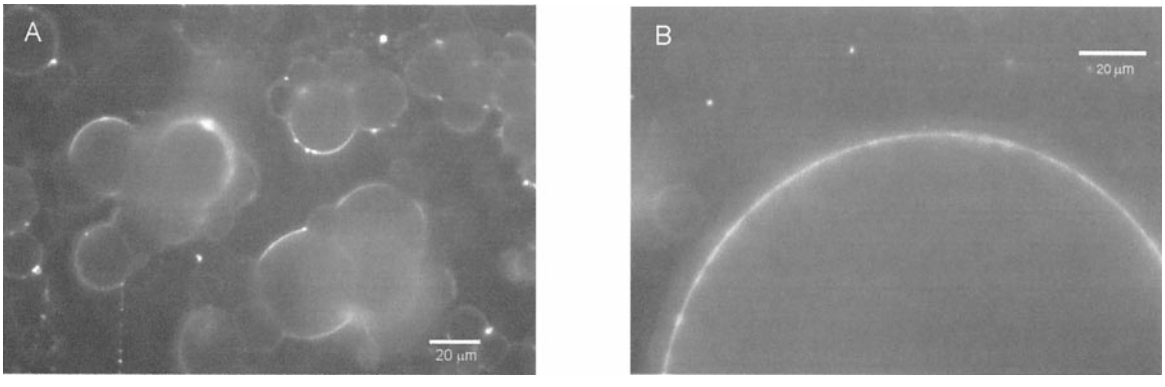

FIGURE 2 Lipid mixing occurs during interaction of WAE-coupled vesicles with GUV. WAE-coupled LUV (DOPC/chol/PE-PDP 3.5:1.5:0.25), labeled with 1% *N*-Rh-PE, were mixed with GUV (DOPC/DOPE/SAINT-2 10:3:1.3) in triple-distilled water and incubated at 37°C. (*A*) 1 to 2 min after addition of the *N*-Rh-PE labeled LUV (size 100 nm), numerous fluorescent spots can been seen on the surface of the GUV, reflecting docking of the WAE-coupled vesicles. (*B*) After 10 to 15 min, most GUV show a continuous ring of fluorescence, which seems to be smooth and homogeneous overall, suggesting that LUV and GUV lipids have mixed. A Zeiss NeoFluor 40×, NA = 0.75 objective was used.

very similar to that previously observed for the kinetics of LUV-LUV fusion (Pécheur et al., 1997).

For LUV-LUV fusion, WAE displayed membrane fusion properties only when covalently coupled to a membrane, whereas free WAE resulted neither in lipid nor contents mixing (Pécheur et al., 1997). The same behavior is observed for GUV-LUV fusion; upon incubation of the peptide-devoid, *N*-Rh-PE-labeled LUV with GUV, no transfer of the fluorescent lipid analogue to the nonlabeled GUV was observed, nor was transfer observed when free peptide was subsequently added (not shown). Rather, transfer of the lipid was only apparent when the GUV were incubated with the peptide-coupled LUV, whereas the presence of free WAE hindered this process, and strongly reduced the GUV-associated yield of fluorescence. Consequently, to accomplish optimal efficiency of interaction, the LUV were purified from the free peptide by gel filtration.

As a result of the fusion, membrane components, initially in the LUV, will finally laterally diffuse in the GUV target membrane, whereas such a diffusion will not be observed upon simple attachment of LUV to GUV. In order to exclude potential defects in the membrane as a consequence of fusion, the morphology of the GUV membrane before and after fusion was investigated by determining the translational mobility of the lipids. Therefore, the lateral diffusion properties of the head group-labeled lipid analogue fluorescein DHPE were examined by FCS (Rigler, 1995; Schwille et al., 1999). From the autocorrelation function $G(\tau)$ of the fluorescence fluctuations in time, one can deduce two properties of the observed molecules: 1) the equilibrium average number of diffusing fluorescent molecules in the laser focal volume, and 2) their diffusion coefficient. To fit $G(\tau)$, we used a two-dimensional Brownian diffusive model (Magde et al., 1972):

$$G(\tau) = \frac{1}{\langle N \rangle}\left[1 + \frac{4D\tau}{r^2}\right]^{-1},$$

where $\langle N \rangle$ is the average number of fluorescent molecules residing in the focal volume element; D, their diffusion coefficient; and r, the radius of the probe area on the focal plane. All measurements were done in a flow chamber (Warner Instrument RC-21) to flush the LUV that did not attach or fuse with GUV, so that freely diffusing LUV in the medium could not interfere with the measurements. Fluorescence fluctuations, measured in several spatial regions of individual GUV and for several different GUV, yielded autocorrelation functions that did not vary significantly. In Fig. 3, the autocorrelation curve is shown for lipid diffusion in the GUV membrane after fusion. Similar curves were obtained for lipid lateral mobility in GUV before fusion (data not shown). The data could be well fitted by the formula given above, showing that after fusion, the lateral dynamics of the lipid molecules in the GUV membrane are identical to those in an unperturbed lipid bilayer, and a diffusion coefficient of 20 $\mu m^2/s$ was calculated. The laser was also focused on GUV surface spots where LUV clustered, as readily discerned by the occasional patchy appearance of fluorescing clusters (Fig. 2 *A*). In this case, longtime scale components were observed in the autocorrelation curves (data not shown), which could not be fitted with the above equation; this is consistent with the immobile nature of the LUV that had docked on but not fused with the GUV.

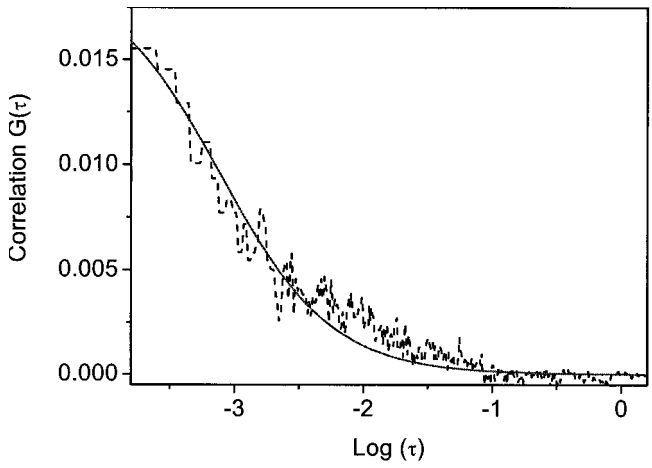

FIGURE 3 Unrestricted diffusion of membrane lipids after LUV-GUV interaction. The lateral diffusion rate of lipids was determined after incubating WAE-coupled vesicles, containing 0.1% fluorescein-DHPE, with GUV, composed as described. The FCS autocorrelation curve was calculated (*dashed line*) from fluorescence bursts detected on the surface of the GUV. The excitation light (488 nm) was focused onto the sample with a 63×, NA = 1.2 water immersion Zeiss C-Apochromat objective and the fluorescence was detected by an avalanche photodiode with a 30-μm pinhole. The fitting curve (*solid line*) was obtained with a one-component two-dimensional diffusive model.

Although lipid mixing is consistent with membrane fusion, it is particularly important to ensure that it represents a genuine fusion process. The next experiments were carried out to support the occurrence of genuine WAE-mediated membrane fusion between LUV and GUV.

Contents mixing between LUV and GUV represents a genuine fusion process

Next to membrane mixing, membrane fusion includes the mixing of aqueous contents of the initially separated membrane-bound compartments. To demonstrate contents mixing for the GUV-LUV system, one needs to take into account that the assay could be severely affected by the dilution of the LUV contents when transferred into the much larger GUV volume. Indeed, a diameter ratio of 1:100 (0.1 μm for LUV and 10 μm for GUV) leads to a volume ratio of $1:10^6$. Consequently, the dilution factor for the contents of each LUV is 10^6, i.e., 100 times larger than for lipid mixing. To determine the transfer of aqueous contents, a highly concentrated fluorescently-labeled dextran solution

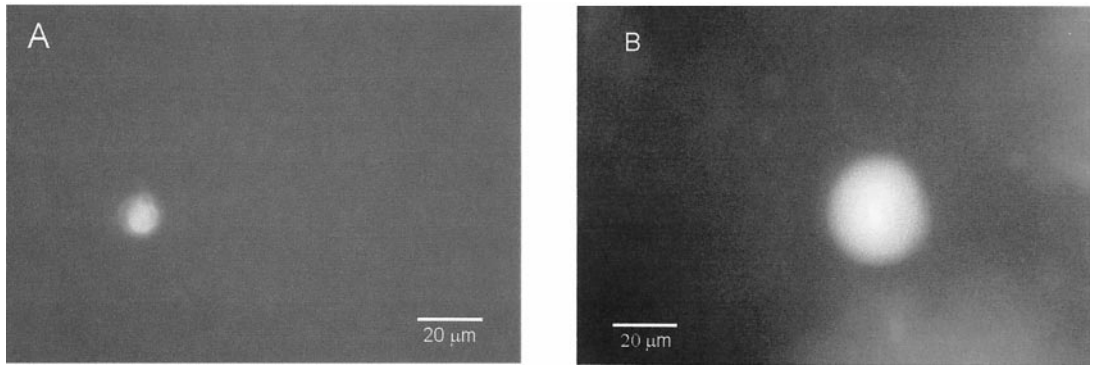

FIGURE 4 WAE-mediated interaction between LUV and GUV represents a genuine fusion event as reflected by contents mixing. (*A*) Contents mixing was assayed by adding WAE-coupled LUV (DOPC/chol/PE-PDP 3.5:1.5:0.25) that contained rhodamine-green labeled dextran (50 mg/ml) to GUV (DOPC/DOPE/SAINT-2 10:3:1.3) in water. The appearance of fluorescence, largely into the smaller GUV, became detectable by fluorescence microscopy after 10 to 15 min at room temperature. (*B*) An alternative procedure was also used which relied on enzymatic cleavage of a fluorogenic substrate. WAE-coupled LUV (DOPC/chol/PE-PDP 3.5:1.5:0.25) containing β-D-galactosidase (2 to 3 units) in Tris-HCl 20 mM, pH 7.6, buffer were added to GUV (DOPC/DOPE/SAINT-2 10:3:1.3) which contained FDG (10 mM final concentration). Fluorescence in the interior compartment of the GUV appears after ~20 to 30 min, resulting from the enzymatic turnover of FDG hydrolysis and consequent release of free fluorescein.

was entrapped within LUV and the appearance of fluorescence in the GUV was followed under the microscope (see Materials and Methods) at conditions identical to those for the lipid mixing assay. After 10 to 15 min, only small GUV with diameters of 5 to 10 μm were found to contain the fluorescent aqueous-soluble dye (Fig. 4 *A*). Apparently, the dilution is a severe drawback to sensitively monitor lumenal contents mixing, using the dextran "dilution" assay. Yet, the data prove that genuine fusion seems to occur in this system.

To reveal that contents mixing also occurred for the larger-sized GUV, we designed a new contents mixing assay. This assay relies on the hydrolytic cleavage of a carbohydrate substrate by a glycosidase. β-Galactosidase was initially entrapped in the LUV, while a fluorescein-conjugated galactopyranoside, which will only fluoresce after enzymatic processing, was enclosed in the GUV. When WAE-coupled LUV and GUV were mixed at fusogenic conditions, the fluorescence emitted by fluorescein, as released upon hydrolysis, could be readily detected inside the GUV. More than 70% of the total amount of GUV became fluorescent after 20 to 30 min (Fig. 4 *B*), indicating that coalescence of lumenal contents had taken place.

Several control experiments were carried out to exclude transfer of enzyme into the GUV by a nonfusion mechanism. Neither upon exogenous addition of the enzyme nor with peptide-devoid but enzyme-containing LUV was any fluorescence detectable within the membrane-bound GUV compartment, even after 3 h of incubation (not shown). These data thus imply that WAE-mediated fusion of LUV with GUV occurs, and that the contents are largely, if not entirely, retained. This shows that WAE-mediated fusion is a nonleaky fusion event. The contents and lipid mixing data are thus in excellent agreement with each other and demonstrate the genuine occurrence of WAE-induced fusion of LUV with GUV.

Quantitative evaluation of the fusion yield

To determine the "fusion efficiency" of the GUV-LUV interaction event, i.e., the number of fused LUV per μm^2 of GUV surface, we performed confocal imaging of GUV after the addition of 100 nm-sized LUV. For calibration, the fluorescence intensity of single LUV was measured (Fig. 5 *A*, *B*), as described in Materials and Methods. These data were then used to interpret the confocal images of GUV after fusion (Fig. 5, *C* and *D*; see Materials and Methods for details). Thus, from the average fluorescence intensity measured in the GUV, we deduced that 6 to 10 LUV were fused per μm^2 of GUV surface.

BR can be reconstituted into GUV by membrane fusion

The ultimate goal of this work was to reconstitute a membrane protein into GUV by means of membrane fusion and to study its dynamics. It is then relevant to evaluate the extent to which the reconstituted protein may interfere with the peptide-coupling to the LUV and with the WAE-membrane fusion event. To avoid potential misfolding of WAE during the detergent-based reconstitution procedure, the coupling reaction of the peptide to the liposomes was performed after protein incorporation. In the absence and presence of the reconstituted protein, the kinetics of peptide coupling and the reaction yields (13% and 12.4%, respectively) were very similar (Fig. 6). We conclude, therefore, that the presence of BR does not interfere with the peptide coupling reaction. Subsequently, the fusion assay was carried out for several LUV/protein concentrations with Alexa Fluor 488-labeled BR. As shown in Fig. 7, *A* and *B*, the images obtained were very similar to those obtained after fusion of *N*-Rh-PE-labeled LUV with GUV (Fig. 2). An

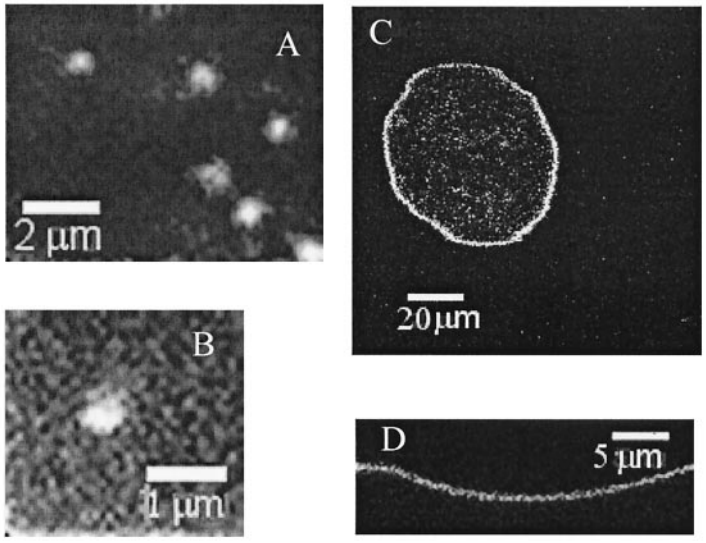

FIGURE 5 The fusion yield per GUV has been quantified. Fluorescence confocal images of WAE-coupled LUV containing 2% fluorescein-DHPE (*A*, *B*) were used to calibrate the fluorescence intensity of single LUV. Subsequently, WAE-mediated fusion was triggered between LUV and GUV. After 10 min at room temperature, a confocal image of the equatorial plane was taken (*C*) and the fluorescence density analyzed (*D*, detail). The excitation beam (λ_{ex} 488 nm) was focused onto the sample with a 63×, NA = 1.2 water immersion Zeiss C-Apochromat objective and the fluorescence was detected by an avalanche photodiode with a 15-μm pinhole. The recorded intensity was correlated with that per LUV, and the number of LUV that contributed to this intensity was thus calculated.

overall diffuse and homogeneous fluorescence signal was visible in the GUV bilayer 10 to 15 min after their mixing with the proteoliposomes. This is a strong indication for an efficient transfer of a significant amount of BR into the GUV membrane. Only at very high protein concentrations (500 μg/ml) could some lysis of the GUV be observed 1–2 h after the injection of the proteoliposomes (not shown).

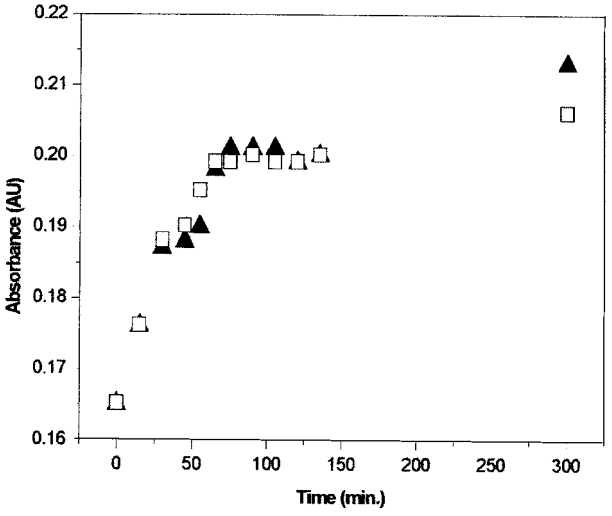

FIGURE 6 The WAE-coupling efficiency is not affected by the presence of reconstituted membrane protein. WAE is covalently coupled to PE-PDP, which causes the release of 2-mercaptopyridine, measured spectrophotometrically at 343 nm. The coupling efficiency to LUV (DOPC/chol/PE-PDP 3.5:1.5:0.25) is shown (▲), as well as the coupling efficiency obtained for LUV in which BR had been reconstituted (50–500 μg/ml) (□).

To further characterize the interaction of the BR-reconstituted LUV with the GUV, the following experiments were carried out: 1) free Alexa 488, added to peptide-devoid LUV and to GUV, showed that the fluorophore did not interfere with vesicle-vesicle interaction; 2) WAE-devoid but BR-containing LUV did associate with the GUV, resulting in a patchy fluorescence (Fig. 7, *C* and *D*, *arrows*); however, at these conditions, fusion did not occur, given the domain-restricted localization of the labeled BR at the GUV surface (compare 7, *A* and *B* vs. 7, *C* and *D*). Although nonspecific electrostatic interaction between the hydrophilic charged residues of BR and the target membrane can trigger GUV-LUV interaction, these data indicate that membrane merging between both vesicle populations solely relies on the action of the fusogenic peptide coupled to LUV. Nonspecific translocation of BR between LUV and GUV can also be excluded.

BR retains its proton pumping activity in GUV

Next, it was of interest to demonstrate functional membrane reconstitution of BR into GUV. The fluorescent pH-sensitive probe pyranine was encapsulated into GUV without removing the nonentrapped probe. At these conditions, a homogenous and diffuse fluorescence image is seen in the fluorescence microscope that does not discriminate between fluorescence derived from either en-

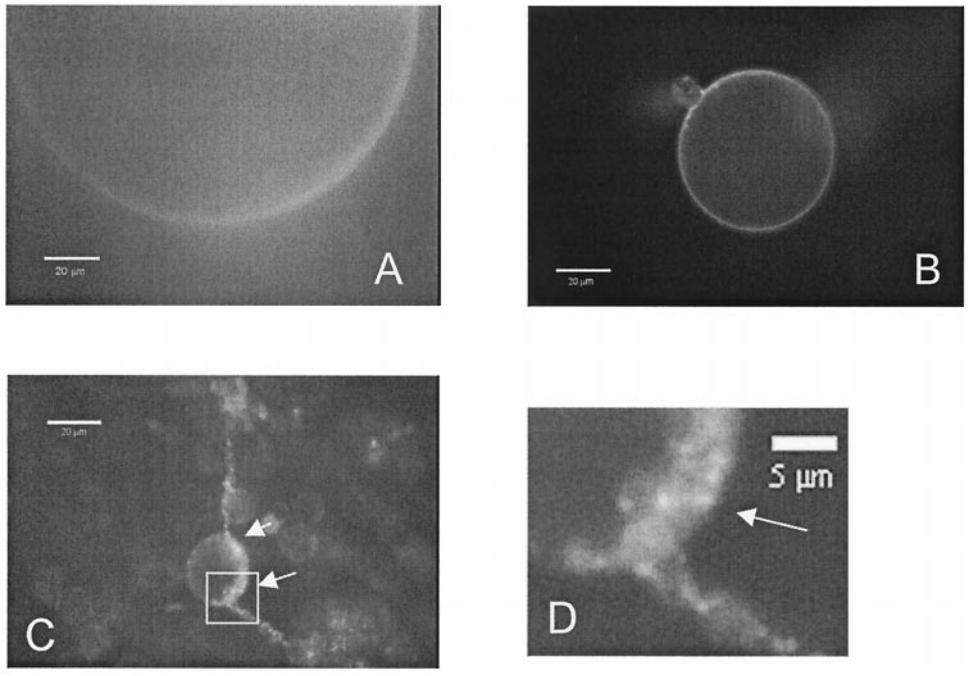

FIGURE 7 WAE-induced fusion mediates the BR transfer into GUV target membranes. The translocation is monitored by protein-lipid mixing, as assayed by fluorescence microscopy. Alexa Fluor 488-labeled BR (50 μg/ml) was reconstituted into LUV. WAE was then coupled to the vesicles and incubated with GUV. Note the presence of the continuous ring of fluorescence, associated with GUV after fusion (*A*, *B*). By contrast, BR-reconstituted, WAE-devoid LUV associated with GUV, showing a typical clustered appearance of bound, but nonfused LUV (*C*, *arrows*, and *D*, detail).

trapped or nonentrapped dye. Hence, fluorescence from inside and outside the GUV is not distinguishable. After activation of BR (see Materials and Methods), protons are pumped into the aqueous GUV space and, as a result, the pyranine fluorescence will decrease (Fig. 8). Quenching occurred in >70% of the total fraction of vesicles present and was strictly dependent on the presence of BR, as no decrease of fluorescence occurred inside the GUV in the absence of BR. It should be noted that photobleaching of pyranine during the course of the experiment does not interfere with the measurements, as only the difference in fluorescence quantum yield between the bulk medium and the lumen of the GUV is relevant to the detection of BR activity. These results imply that BR can be functionally reconstituted into GUV and that the insertion occurs with a preferential orientation (inside-out).

BR undergoes unrestricted lateral diffusion in GUV

After having demonstrated that BR is stably and correctly inserted into the GUV's bilayer, we investigated its trans-

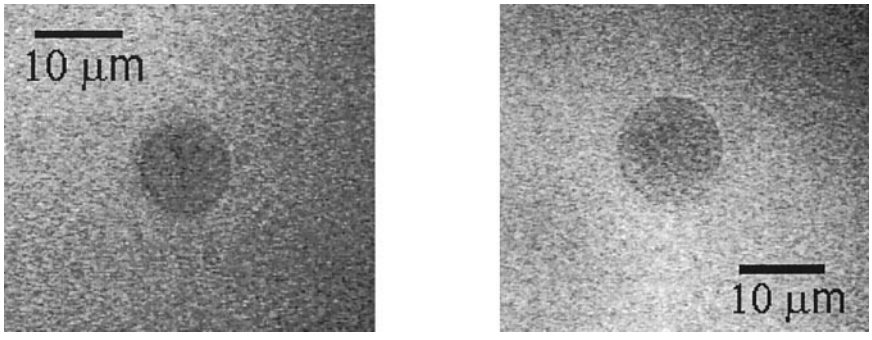

FIGURE 8 BR is functionally reconstituted into GUV. GUV were prepared in a medium containing the pH-sensitive dye pyranine. BR was reconstituted into GUV as described in the legend to Fig. 7. The protein was then activated as described in Methods, causing the time-dependent translocation of protons across the GUV membrane into its aqueous space, where a decrease in pH will quench entrapped pyranine. The decrease in "encapsulated" fluorescence allows to distinguish the circumference of the GUV and assays BR functional reconstitution. Note that GUV are not distinguishable from background fluorescence when the same experiment is carried out with GUV that do not contain BR.

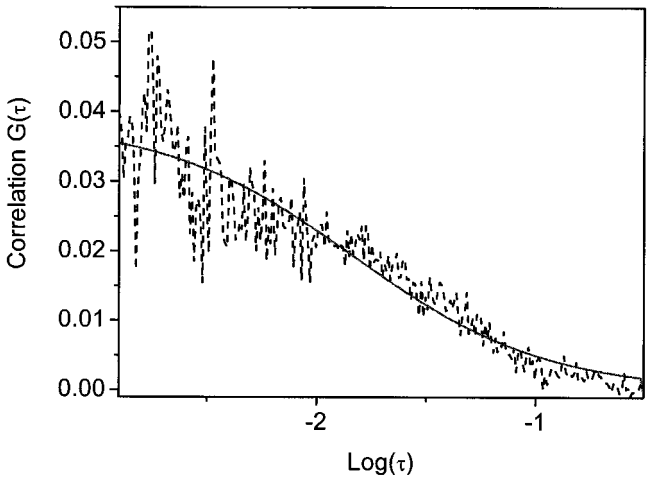

FIGURE 9 FCS autocorrelation curve, calculated (*dashed line*) from fluorescence bursts detected for Alexa Fluor-labeled BR in GUV. The excitation light (488 nm) was focused onto the sample with a 63×, NA = 1.2 water immersion Zeiss C-Apochromat objective and the fluorescence was detected by an avalanche photodiode with a 30-μm pinhole. The fitting curve (*solid line*) was obtained with one-component, two-dimensional diffusion model.

lational diffusion behavior by FCS. The resulting autocorrelation decay could be fitted with a single-component function such as for the lipid lateral diffusion (Fig. 9). BR diffuses in GUV with a lateral diffusion coefficient of $\sim$1.2 $\mu m^2/s$.

DISCUSSION

In this work, we present a protocol to reconstitute integral membrane proteins into GUV via peptide-induced fusion. The protein dynamics and functionality in the close-to-native environment of the GUV can then be studied by optical microscopy. As shown here for the model system BR, it is possible to determine the lateral mobility of membrane proteins by FCS. Moreover, membrane translocation controlled by a protein can be readily studied since the resulting changes in the lumen of the cell-like GUV can be detected by optical microscopy. This feature is demonstrated here by studying the proton pumping activity of BR. To use the full potential of this protocol, it is necessary to exclude any artifacts during the reconstitution. Therefore, all essential steps in the reconstitution process were characterized by confocal microscopy and FCS. The reconstitution procedure described is, in general, applicable for single-molecule optical microscopy studies of lateral and rotational mobility, folding and association-dissociation equilibria of individual protein molecules (Xie and Trautman, 1998; Xie and Lu, 1999; Harms et al., 1999; Deniz et al., 2000). Although the development of such techniques has been reported recently for in vivo systems (Schutz et al., 2000), it is also desirable to study protein dynamics and functionality in vitro. In these experiments, the well-defined molecular environment can be varied systematically, thus providing a better and more accurate insight into the protein structure/function relationship and the lipid/protein interaction.

GUV are a priori excellent membrane model systems because they provide free-standing bilayers and a chemically well defined composition, which, to a certain extent, can be varied. The major biologically relevant phospholipids such as PC, PE, PG and PS, with or without cholesterol do allow electroformation of GUV (Angelova and Dimitrov, 1986; Menger and Angelova 1998; Angelova et al., 1992).

For many applications, GUV surpass alternative in vitro systems. LUV, for instance, cannot be studied by single-molecule optical microscopy because it is not possible to expose only a section of the LUV to the light of the microscope as can be done with GUV. In contrast to monolayers, GUV resemble more closely the natural bilayer membrane structure. They also surpass supported planar bilayers, which suffer from severe artifacts because of the presence of a rigid support. It is known that the support, typically glass or quartz, interacts with the exposed soluble domains and thereby lowers the mobility of the proteins in the membrane (Hinterdorfer et al., 1994; Salafsky et al., 1996). The insertion of soft polymer cushions between the lipid bilayer and the support improves the quality and reduces the artifacts in the case of particular classes of proteins such as membrane-bound and peripheral membrane-proteins, but the limitations for applications to transmembrane proteins still remain (Wagner and Tamm, 2000). Until now, the inability to reconstitute membrane proteins in their bilayers has been a major drawback in the application of GUV for in vitro studies of protein dynamics. The intrinsic fragility of the vesicles precludes the manipulations required for reconstitution, while the critical electroformation procedure, necessary for vesicle assembly, is harmful to the protein.

Here, we present a novel procedure for protein reconstitution in GUV which avoids these major problems by exploiting the possibilities of peptide-induced fusion. First, we show that WAE-induced GUV-LUV fusion, which is reported here for the first time, does not introduce changes in the membrane morphology. As it is shown by FCS, the lipid mobility of 20 $\mu m^2/s$, which is consistent with previous data for lipid lateral mobility measured by SPT (Sonnleitner et al., 1999), is unchanged after fusion. It is also demonstrated that the fusion does not lead to a destabilization of the membrane. No substantial leakage of contents was observed in the contents mixing assays, as shown by the retention of both fluorescent dextran and the much smaller fluorescein dye (Fig. 4, *A* and *B*, respectively). The latter feature of the fusion process is essential for membrane transport studies where the lumen of GUV and LUV are filled with probes used for optical microscopic assays. In general, these stud-

ies can be quite challenging because of the large GUV lumen and the resulting low concentrations. In this work, the dilution problem is solved by an enzyme-based assay, in which the high turnover of a single enzyme successively activates the fluorescence of a large number of dye molecules, released by cleavage of the substrate. This mechanism, which increases the experimental sensitivity by orders of magnitude, can be applied to future fluorescence assays.

Presumably, the well defined GUV-LUV fusion occurs analogously to the LUV-LUV fusion previously studied (Pécheur et al., 1997, 1999). For the latter system, fusion proceeds via a controlled stalk-pore mechanism, involving the shallow penetration of (part of) the α-helical WAE structure (Martin et al., 1999). Most importantly, during LUV-LUV fusion, WAE's entry into the target membrane does not cause destabilization of the merging membranes (Pécheur et al., 1997). This feature, in particular, makes WAE a very useful fusogen in fusion-mediated reconstitution, involving relatively fragile GUV.

This microscopic model for GUV-LUV fusion is also supported by optical microscopy. The first step in fusion is an extensive docking of LUV on the GUV surface, which can be clearly observed by a patchy, irregular fluorescence pattern surrounding the GUV periphery (Fig. 2 *A*). After docking, merging of the two membranes occurred within minutes, thus proceeding with a kinetics similar to that for LUV-LUV fusion (Pécheur et al., 1997). The fusion resulted in a smooth and homogeneous fluorescence because of diffusion of the fluorescent lipids in the GUV's membrane as shown in Fig. 2 *B*. Previous studies of LUV-LUV fusion showed that WAE-induced fusion does show a target membrane lipid-preference for fusion in terms of efficiency, but the fusogenic activity per se is not critically dependent on that composition (Pécheur et al., 1999). This also holds for GUV-LUV fusion, since LUV fuse with GUV with different amounts of neutral and anionic, bilayer and non-bilayer forming lipids, with or without cholesterol (unpublished results). Therefore, this approach allows the application of a wide variety of GUV lipid compositions.

Subsequently, we quantified the GUV-LUV fusion efficiency by fluorescence intensity analysis of confocal images of GUV. It is shown that 6 to 10 (100-nm–sized) LUV had fused per μm^2 of GUV's surface, implying that, on average, 10,000 LUV merge per GUV with a size of 20 μm (Fig. 5). The large number of fusion events indicates that a substantial amount of membrane proteins can be transferred in this way. The lipid composition of GUV after fusion then corresponds for ~80% to that of the original GUV and for ~20% to that of LUV.

Having characterized the fusion process, we now discuss the reconstitution of BR via GUV-LUV fusion. First, BR is reconstituted into LUV (Rigaud et al., 1988). The right orientation of BR in the LUV membrane, which is essential for optimal activity, is obtained by reconstituting monomeric BR into preformed liposomes. Then, the BR-containing LUV are fused with GUV, as before. The experiments show that the presence of BR in the LUV did not interfere with WAE-induced fusion. The enzyme-based assay for contents mixing was repeated with BR-containing LUV and gave results very similar to those obtained in the absence of the membrane protein (data not shown, cf. Fig. 4). Thus, also with the protein, fusion occurs without significant leakage and involves both lipid and aqueous contents mixing. After fusion, BR does not form aggregates visible under the microscope, as shown in Fig. 7, *A* and *B*, where the fluorescently labeled BR is smoothly distributed over the entire membrane. From the fusion efficiency discussed above, it can be deduced that 10,000 to 150,000 BR molecules are inserted into a GUV, depending on the concentration of BR in LUV. After reconstituting this amount of proteins, the functionality was assayed by monitoring the change of pH in the lumen of the GUV because of the proton-pumping activity of BR.

Finally, the mobility of BR, determined by FCS, was found slower than that of the lipids, as expected for particles of higher mass. The unrestricted Brownian motion of BR in GUV is characterized by a single diffusion coefficient of 1.2 $\mu m^2/s$. This information can be only reliably obtained with free-standing bilayers, such as GUV, whereas, in supported bilayers, large fractions of proteins are immobile or partially mobile because of interactions of the protein residues with the support or the polymeric cushion between the support and the membrane (Wagner and Tamm, 2000). Interestingly, further FCS experiments, not reported here, indicated that BR changes its lateral mobility upon the activation of the photocycle in a reversible manner. Upon photoactivation, the mobility slowed down and increased again to control values when photoactivation was abrogated. Possibly, this switching between different mobilities is related to a change in the monomer/oligomer equilibrium when the protein becomes light-activated.

In conclusion, the technique described here allows reconstitution of membrane proteins other than BR into GUV, provided that they can be effectively incorporated into LUV. We recently succeeded in applying the reconstitution technique to protein complexes involved in protein translocation machineries. A different lipid composition than that used for BR was required for this. This novel approach to reconstitute proteins into GUV as mediated by a fusion mechanism should prove to be extremely useful in addressing fundamental questions regarding protein function and oligomeric structure.

The Department of Electron Microscopy (Head Prof. Alain Brisson) is acknowledged for making available their facilities. We are grateful for Prof. Dr. Bert Poolman for helpful discussions and critical reading of the manuscript. F. de Haan contributed to this work by providing the software for the data acquisition. We acknowledge the financial support obtained from the European Commission (contract ERBFMBICT972580 and, partially, contract BIO4-CT97–2191 (DH)).

REFERENCES

Angelova, M. I., and D. S. Dimitrov. 1986. Liposome electroformation. *Faraday Discuss. Chem. Soc.* 81:303–308.

Angelova, M. I., S. Soléau, P. Méléard, J. F. Faucon, and P. Bothorel. 1992. Preparation of giant vesicles by external AC electric fields. Kinetics and applications. *Progr. Colloid. Polym. Sci.* 89:127–131.

Camilli, P. D., and G. Warren. 1999. Membranes and sorting, getting there. *Curr. Opin. Cell Biol.* 11:423–424.

Dencher, N. A., and M. P. Heyn. 1982. Preparation and properties of monomeric bacteriorhodopsin. *Methods Enzymol.* 88:5–10.

Deniz, A. A., T. A. Laurence, G. S. Beligere, M. Dahan, A. B. Martin, D. S. Chemla, P. E. Dawson, P. G. Schultz, and S. Weiss. 2000. Single-molecule protein folding: diffusion fluorescence resonance energy transfer studies of the denaturation of chymotrypsin inhibitor 2. *Proc. Natl. Acad. Sci. U.S.A.* 97:5179–5184.

Dimitrov, D. S., and M. I. Angelova. 1988. Lipid swelling and liposome electroformation mediated by electric fields. *Bioelectrochem. Bioenerg.* 19:323–333.

Eigen, M., and R. Rigler. 1994. Sorting single molecules: Application to diagnostics and evolutionary biotechnology. *Proc. Natl. Acad. Sci. U.S.A.* 91:5740–5747.

Ghosh, R. N., and W. W. Webb. 1994. Automated detection and tracking of individual and clustered cell surface low density lipoprotein receptor molecules. *Biophys. J.* 66:1301–1318.

Harder, T., and K. Simons. 1997. Caveolae, DIGs, and the dynamics of sphingolipid-cholesterol microdomains. *Curr. Opin. Cell. Biol.* 9:534–542.

Harms, G. S., M. Sonnleitner, G. J. Shutz, H. J. Gruber, and T. Schmidt. 1999. Single-molecule anisotropy imaging. *Biophys. J.* 77:2864–2870.

Hinterdorfer, P., G. Barber, and L. K. Tamm. 1994. Reconstitution of membrane fusion sites. A total internal reflection fluorescence microscopy study of influenza hemmaglutinin-mediated membrane fusion. *J. Biol. Chem.* 269:20360–20368.

Magde, D., E. Elson, and W. W. Webb. 1972. Thermodynamic fluctuations in a reacting system-measurement by fluorescence correlation spectroscopy. *Phys. Rev. Lett.* 29:705–708.

Martin, I., E.-I. Pécheur, J.-M. Ruysschaert, and D. Hoekstra. 1999. Membrane fusion induced by a short fusogenic peptide is assessed by its insertion and orientation into target bilayers. *Biochemistry.* 38: 9337–9347.

Mathivet, L., S. Cribier, and P. F. Devaux. 1996. Shape changes and physical properties of giant phospholipid vesicles prepared in the presence of an AC electric field. *Biophys. J.* 70:1112–1121.

Menger, F. M., and M. I. Angelova. 1998. Giant vesicles: imitating the cytological processes of cell membranes. *Acc. Chem. Res.* 31:789–797.

Oesterhelt, D., and W. Stoeckenius. 1974. Isolation of the cell membrane of *Halobacterium halobium* and its fractionation into red and purple membrane. *Methods Enzymol.* 31:667–678.

Pécheur, E.-I., D. Hoekstra, J. Sainte-Marie, L. Maurin, A. Bienvenue, and J. R. Philippot. 1997. Membrane anchorage brings about fusogenic properties in a short synthetic peptide. *Biochemistry.* 36:3773–3781.

Pécheur, E.-I., J. Sainte-Marie, A. Bienvenue, and D. Hoekstra. 1999. Lipid headgroup spacing and peptide penetration, but not peptide oligomerization, modulate peptide-induced fusion. *Biochemistry.* 38:364–373.

Philippot, J., S. Mutaftschief, and J. P. Liautard. 1983. A very mild method allowing the encapsulation of very high amounts of macromolecules into very large (100 nm) unilamellar liposomes. *Biochim. Biophys. Acta.* 734:137–143.

Rigaud, J. L., M. T. Paternostre, and A. Bluzat. 1988. Mechanisms of membrane protein insertion into liposomes during reconstitution procedures involving the use of detergents. 2. Incorporation of the light-driven proton pump bacteriorhodopsin. *Biochemistry.* 27:2677–2688.

Rigler, R. 1995. Fluorescence correlations, single molecule detection and large number screening applications in biotechnology. *J. Biotechnol.* 41:177–186.

Sackmann, E. 1996. Supported membranes: scientific and practical applications. *Science.* 271:43–48.

Salafsky, J., J. T. Groves, and S. G. Boxer. 1996. Architecture and function of membrane proteins in supported bilayers: a study with photosynthetic reaction centers. *Biochemistry.* 35:14773–14781.

Schmidt, T., G. J. Schutz, W. Baumgartner, H. J. Gruber, and H. Schindler. 1995. Characterization of photophysics and mobility of single molecules in a fluid lipid membrane. *J. Phys. Chem.* 99:17662–17668.

Schmidt, T., G. J. Schutz, W. Baumgartner, H. J. Gruber, and H. Schindler. 1996. Imaging of single molecule diffusion. *Proc. Natl. Acad. Sci. U.S.A.* 93:2926–2929.

Schutz, G. J., G. Kada, V. P. Pastushenko, and H. Schindler. 2000. Properties of lipid microdomains in a muscle cell membrane visualized by a single molecule microscopy. *EMBO J.* 19:892–901.

Schwille, P., J. Korlach, and W. W. Webb. 1999. Fluorescence correlation spectroscopy with single-molecule sensitivity on cell and model membranes. *Cytometry.* 36:176–182.

Simons, K., and E. Ikonen. 1997. Functional rafts in cell membranes. *Nature.* 387:569–572.

Simons, K., and D. Toomre. 2000. Lipid rafts and signal transduction. *Nature Rev. Mol. Cell Biol.* 1:31–39.

Sonnleitner, A., G. J. Schutz, and T. Schmidt. 1999. Free Brownian motion of individual lipid molecules in biomembranes. *Biophys. J.* 77: 2638–2642.

Tamm, L. K., and E. Kalb. 1993. Microspectrofluorometry on supported planar membranes. *In* Molecular Luminescence Spectroscopy, Part 3. S. G. Schulmann, editor. John Wiley and Sons, New York. 253–305.

Van Voorst, F., and B. de Kruijff. 2000. Role of lipids in the translocation of proteins across membranes. *Biochem. J.* 347:601–612.

Wagner, M. L., and L. K. Tamm. 2000. Tethered polymer-supported planar lipid bilayers for reconstitution of integral membrane proteins: silane-polyethyleneglycol-lipid as a cushion and covalent linker. *Biophys. J.* 79:1400–1414.

Woude, I. v. d., A. Wagenaar, A. A. P. Neekel, N. B. ter Beest, N. H. J. Ruiters, J. B. F. N. Engberts, and D. Hoekstra. 1997. Novel pyridinium surfactants for efficient, nontoxic in vitro gene delivery. *Proc. Natl. Acad. Sci. U.S.A.* 94:1160–1165.

Xie, X. S., and H. P. Lu. 1999. Single-molecule enzymology. *J. Biol. Chem.* 274:15967–15970.

Xie, X. S., and J. K. Trautman. 1998. Optical studies of single molecules at room temperature. *Annu. Rev. Phys. Chem.* 59:441–480.

Zimmerberg, J., S. S. Vogel, and L. V. Chernomordick. 1993. Mechanisms of membrane fusion. *Annu. Rev. Biophys. Biomol. Struct.* 22:433–466.